

Growth of metal and metal oxide nanowires driven by the stress-induced migration

Mingji Chen, Yumei Yue, and Yang Ju^{a)}

Department of Mechanical Science and Engineering, Nagoya University, Furo-cho, Chikusa-ku, Nagoya 464-8603, Japan

(Received 13 February 2012; accepted 16 April 2012; published online 18 May 2012)

High quality Al and CuO nanowires are fabricated by simply heating the Al and Cu samples in air. Although the experimental operations and the stress-induced migration processes are quite similar, the causes of the driving forces and the growth mechanism are completely different. For the growth of Al nanowires, the driving force is determined to be the compressive stresses caused by the thermal expansion mismatch between Al film and Si substrate, and the growth mechanism is proposed to be the extrusion of atoms from the bases of nanowires (EAFB). For the growth of CuO nanowires, the driving force is determined to be the compressive stresses caused by the formation of Cu oxide layers, and the growth mechanism is proposed to be the formation of oxide molecules on surfaces of the nanowires (FOOS). The direct experimental observations of both EAFB and FOOS are presented. It is also demonstrated that stress distribution on the macroscopic level, which is caused by thermal or mechanical manipulation, can also influence the growth of CuO nanowires, which makes it prospective to control the growth of metal oxide nanowires by designing the stress distribution within the sample from which the nanowires are generated. © 2012 American Institute of Physics. [<http://dx.doi.org/10.1063/1.4718436>]

I. INTRODUCTION

Metal oxide nanowires, such as CuO and ZnO nanowires, were demonstrated to have fantastic applications in solar cells,¹ field emitters,² toxic gas detectors,³ etc. Compared with traditional semiconductor such as Si and GaAs, metal oxides are more plentiful and low-cost with low toxicity and good environmental acceptability, which makes devices based on metal oxide nanowires more prospective. Synthesis of dense CuO nanowires by heating the high-purity Cu samples was reported in 2002.⁴ This method was followed by many researchers^{5–12} due to the single crystal or bicrystal structures of the resultant nanowires as well as its simple requirements on equipments and experimental conditions. Moreover, it can serve as an effective method for positioned growth of well aligned metal oxide nanowires¹¹ and thus is potential for integrating nanowires into devices.²

In fact, growth of metal oxide nanowires or nano-whiskers during the heating process of metals has been observed since 1950s.^{13–15} Cu, Zn, and Fe have been reported to be three of the most typical metals from which CuO,^{4,14} ZnO,^{14,16} and Fe₂O₃ (Refs. 14 and 17) nanowires can be steadily generated, respectively. The word “steadily” here indicates that the metal oxide nanowires can be generated during heating of the high-purity metal samples, regardless of the types and dimensions of samples. On the other hand, Al,^{18–20} Ag,²¹ and Bi (Refs. 22–24) nanowires have only been reported to be generated by heating their film-substrate systems.

Beside plenty of synthesis and application researches, the growth mechanism has also been studied. Some research-

ers tended to believe that the nanowires were formed due to the extrusion of metal atoms driven by the compressive stresses in the samples.^{18–25} In this case, the nanowires were supposed to grow from their bases. On the other hand, growth of metal oxide nanowires was also interpreted as the result of thermal oxidation process.^{5–10,16,17,26} In this case, the nanowires were supposed to grow by adding oxide molecules on their tips, which was quite different from the extrusion mechanism. Therefore, up to now, there is still no generally accepted interpretation on fabricating metal and metal oxide nanowires by simply heating the high-purity metal samples.

In this paper, we present reasonable interpretations on the growth mechanism of metal and metal oxide nanowires. The growth of nanowires is driven by stress-induced migration, but the growth mechanism can be classified into two different types, namely, the extrusion of atoms from the bases of nanowires (EAFB) and formation of oxide molecules on surfaces of the nanowires (FOOS). Although growth of metal oxide nanowires from their tips was supported by many researchers,^{5,6,8–10,16,17,26} the experimental observation of FOOS was rarely reported. Here, we present direct experimental observation on the growth process of both metal and metal oxide nanowires to support our interpretations on the different types of growth mechanism. Although it is believed that gas flow can affect the growth of nanowires,⁵ in this paper, we only focus on the growth of nanowires in air. It is shown that the metal oxide nanowires can grow very well even without a closed environment and specific gas flow.

II. EXPERIMENT

Growth of Al and CuO nanowires was carried out in this study on both the metal film-substrate systems and metal

^{a)}Author to whom correspondence should be addressed. Electronic mail: ju@mech.nagoya-u.ac.jp. Tel.: +81-52-789-4672. Fax: +81-52-789-3109.

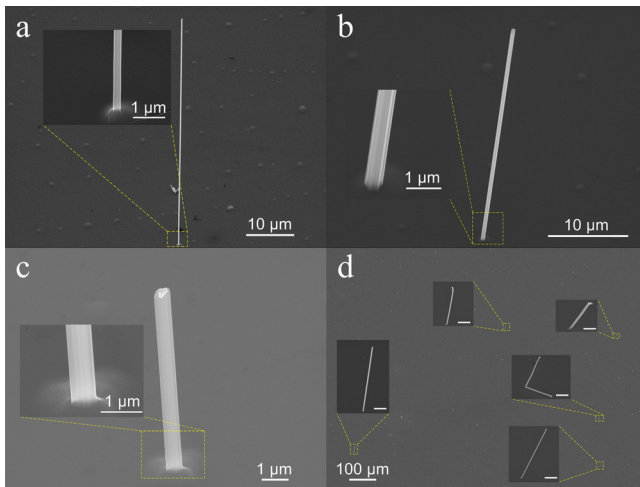


FIG. 1. Al nanowires growing after heating at 240 °C for 4.5 h. (a) A nanowire with high aspect ratio. (b) A typical Al nanowire with diameter of 500 nm. (c) A thick and relatively short nanowire. (d) Number density of the Al nanowires, the scale bars in all the insets are 5 μm .

foils. The Al and Cu foils utilized were 250 and 300 μm thick, respectively, and the purity was 99.9%. Al film with thickness of 200 nm was deposited directly on the Si substrate by the electron beam evaporation (EBE). For Cu film, a 60 nm thick Ta layer was first deposited on the Si substrate to serve as the adhesive layer. Then, a 400 nm thick Cu film was deposited on the Ta adhesive layer by EBE. Patterned Cu film samples were also prepared by implementing the optical lithography before deposition of the Ta layer and a 400 nm thick Cu film. The patterned Cu film was in the shape of a flat column with diameter and thickness of 10 μm and 400 nm, respectively.

In order to grow nanowires, the metal foils and films were heated on a ceramic heater in air. The ceramic heater was powered by a voltage source, and the heating temperature could be well controlled by adjusting the supplied voltage. The Al foils and films were heated at temperatures from 200 to 300 °C, while the Cu foils and films were heated at temperatures from 250 to 450 °C.

The samples with nanowires were observed by scanning electron microscopy (SEM). Individual nanowires were also separated from the substrates and collected on the observation grid of the transmission electron microscope (TEM). The results of electron energy loss spectroscopy (EELS) together with the TEM images were obtained from the individual nanowires.

III. RESULTS AND DISCUSSION

A. Growth of Al nanowires dominated by the EAFB mechanism

Al nanowires can grow well only on the Al film samples at a narrow temperature range between 200 and 240 °C. Heating Al foils did not generate nanowires, while heating Al films at a temperature out of the aforementioned range only generated nanowires occasionally on the film surfaces. Heating Al films at 240 °C for 4.5 h gave the following results. The number density of Al nanowires was approximately 10^3 cm^{-2} . The length and diameter of the Al nanowires were always 10–50 μm and 200–500 nm, respectively, as shown in Fig. 1. The highest aspect ratio was around 200–300. Shorter nanowires and nanowires with diameters of smaller than 200 nm or larger than 500 nm were also found occasionally.

The growth process of Al nanowires was observed and presented in Figs. 2(a)–2(d). As shown in Figs. 2(a) and 2(b), the tip of nanowire did not change during the growth process. Thus, it was demonstrated by direct experimental observation that the Al nanowires grew from their bases. The straight and facet nanowire surfaces shown in Figs. 1 and 2 corresponded with the shapes of the holes surrounding the bases of nanowires. It can also be seen from Fig. 2(c) that the morphology of the nanowire tip corresponded well with that of the local protective layer, which was peeled off from the sample surface (Fig. 2(d)). All these evidences support the conclusion that the growth mechanism of Al nanowires belongs to EAFB.

When the Al film-substrate system was heated in air, in-plane biaxial compressive stresses were generated in Al film

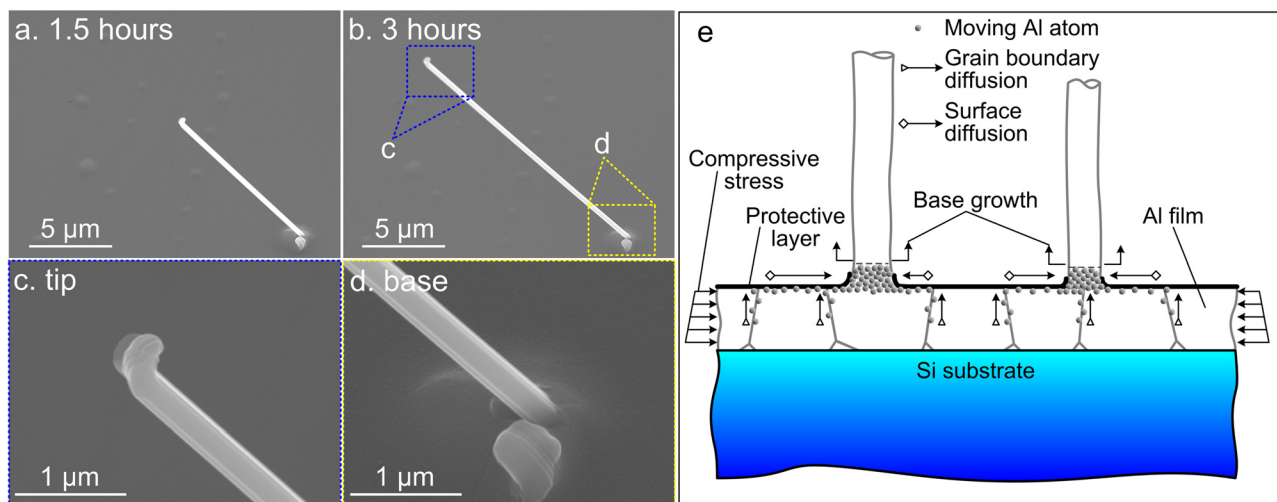


FIG. 2. Growth process of the Al nanowire. (a) After heating for 1.5 h. (b) After heating for 3 h. (c) The tip of nanowire. (d) The base of nanowire. (e) Illustration of the EAFB mechanism for Al nanowire growth.

due to the thermal expansion mismatch between the film and the substrate. Since the surface of Al film was covered by a thin protective layer, either a deposited protective layer¹⁸ or the natural oxide layer (as in this study), the compressive stresses could not be relieved freely on the film surface. The Al atoms tended to migrate from more compressive areas to less compressive ones in the form of stress-induced grain boundary diffusion and surface diffusion (Fig. 2(e)). When plenty of Al atoms accumulated on some sites near the film surface, it was resulted that the local protective layers were broken through and nanowires were extruded from these broken sites. Thus, the shapes of the nanowire surfaces should follow the shapes of the holes from which they were extruded. This is the reason why the facet nanowire surfaces corresponded with the shapes of the holes surrounding the bases of nanowires. Then, the continuous growth of Al nanowires was supported by the continuously coming atoms due to stress-induced migration. In the whole process, the stress gradient induced by the thermal expansion mismatch between Al film and Si substrate acted as a dominant factor. That is the reason why Al nanowires could not be generated by heating Al foil in air.

B. Growth of CuO nanowires dominated by the FOOS mechanism

SEM images of CuO nanowires growing on Cu films and Cu foils, which were heated at the temperature from 300 to 450 °C for 2 h were shown in Figs. 3 and 4, respectively. It can be seen from these two figures that CuO nanowires were generated on both film and foil samples when heating the samples in air at a proper temperature range. CuO nanowires growing on Cu foils after being heated at 400 °C for 2 h were even longer than those growing on Cu films under the same condition. This is quite different from the case of Al nanowires. The number density of CuO nanowires may reach up to 10^6 times larger than that of the Al nanowires. Besides, for CuO nanowires growing on both film and foil samples, it was observed that the diameter of nanowires increased with the temperature obviously. From Figs. 3 and 4, the optimum

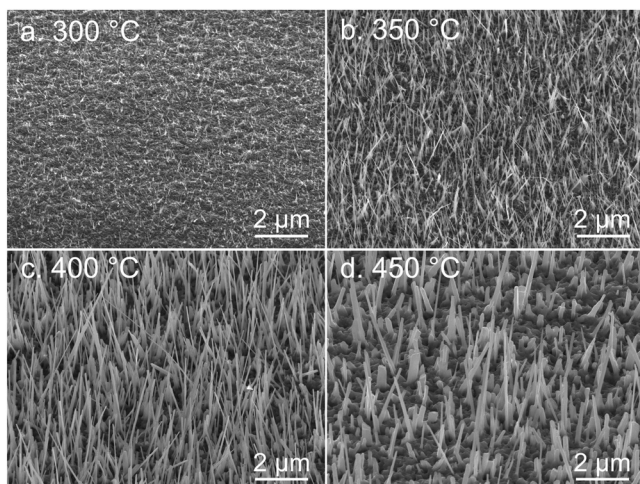


FIG. 3. CuO nanowires growing on the Cu films after being heated at different temperatures of (a) 300 °C, (b) 350 °C, (c) 400 °C, and (d) 450 °C for 2 h.

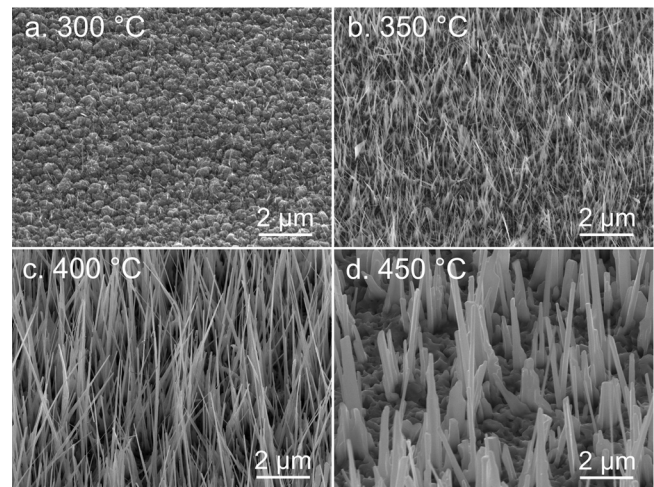


FIG. 4. CuO nanowires growing on the Cu foils after being heated at different temperatures of (a) 300 °C, (b) 350 °C, (c) 400 °C, and (d) 450 °C for 2 h.

temperature for CuO nanowire growth was supposed to be around 400 °C, while much thinner nanowires could be generated at 350 °C. For heating temperatures of 300 °C or lower, only thin and short ($\sim 0.5 \mu\text{m}$ long) nanowires could be generated. For heating temperatures of 450 °C or higher, the number density became very low. The data of CuO nanowires growing on Cu films were presented in Table I.

To study the influence of heating time, Cu films were heated at 400 °C for 10, 30, 60, and 120 min, respectively, and the results were presented in Fig. 5. Although the number density was almost unchanged, the length and diameter of CuO nanowires both increased with the heating time. It can be seen from Fig. 6 that the increasing rates of length and diameter were relatively high before the film samples were heated for 30–60 min, and then became much lower. Heating the film samples for more than 2 h no longer improved the growth of CuO nanowires significantly.

Direct observation of growth process of CuO nanowires on the same film sample was also carried out. As shown in the enlarged SEM images in Figs. 7(a) and 7(c), most nanowires were observed to grow directly from the surface grains of the sample. This is quite different from the Al nanowires, which were extruded from holes on the sample surface. Moreover, the shapes and surface morphologies of the CuO nanowires were much more complicated than the Al nanowires. Most of the CuO nanowires were in the shape of a needle, namely, thicker at their bases and thinner at their tips. With the advance of the growth process, branched nanowires (VI in Fig. 7(b)) and nanowires having secondary parts (more narrow parts on the thicker bases, as I and III in Fig. 7(b)) were also observed. Images shown in Figs. 7(b)

TABLE I. Data of CuO nanowires growing on Cu films after being heated at different temperatures for 2 h.

Temperature/°C	300	350	400	450
Number density/ 10^9 cm^{-2}	1.5	1.8	1.5	0.4
Average length/ μm	0.5	1.6	3.5	2.0
Average diameter/nm	15	30	48	100

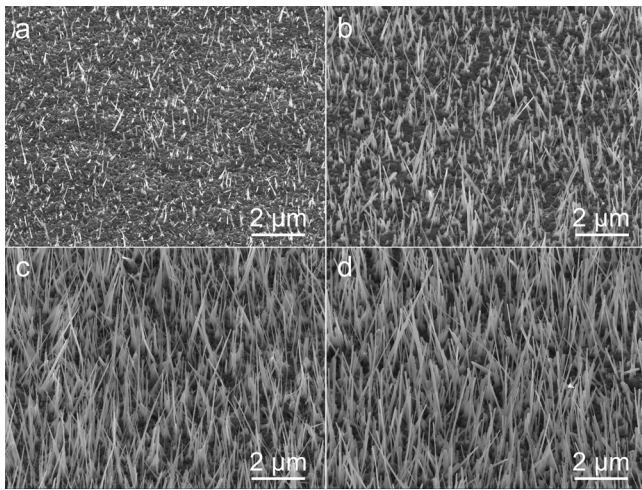


FIG. 5. CuO nanowires growing on the Cu films after being heated at 400 °C for (a) 10 min, (b) 30 min, (c) 60 min, and (d) 120 min.

and 7(d) were taken from the same places as Figs. 7(a) and 7(c), respectively, after the sample had been heated for 20 more minutes. Obvious elongation of the secondary parts (I and III in Fig. 7(b)) and the formation of branched structure (VI in Fig. 7(b)) indicated that the CuO nanowires did not grow from their bases. It has also been observed that many nanowires grew not only longer but also thicker (II, IV in Figs. 7(a) and 7(b) and I, II, III in Figs. 7(c) and 7(d)). These evidences support that the growth of CuO nanowires was implemented by the formation of oxide molecules on surfaces (tips and sidewalls) of the nanowires (FOOS). Although growth of CuO nanowires from their tips were supported by many researchers,^{5,6,8–10,26} the direct experimental observation of FOOS as presented here was rarely reported before.

The driving force for growth of CuO nanowires was proposed to be the compressive stresses generated in the samples during the heating process.^{8,10,25,26} However, regarding to the origin of the compressive stresses, there was still no generally accepted interpretation. Some researchers indicated that the stresses were generated due to the formation of Cu₂O and CuO layers during the heating process,^{8,10,26} while others thought that it was the thermal expansion mismatch between Cu film and Si substrate that induced the compressive stresses in the Cu film.²⁵ According to our experiment results that

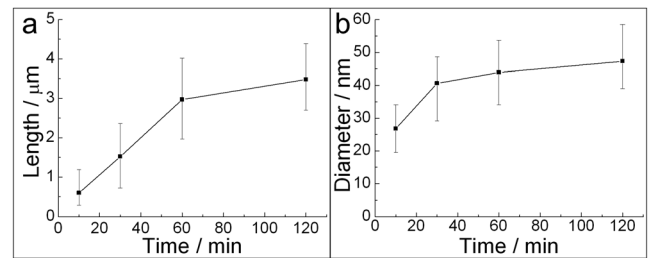


FIG. 6. Curve of (a) length and (b) diameter of CuO nanowires vs the heating time. The Cu nanowires were generated on Cu films at 400 °C.

heating Cu foils also generated CuO nanowires, we believed that the former interpretation was more reasonable.

When the Cu samples were heated in air, two thermodynamically stable oxide layers, namely, Cu₂O and the topmost CuO layers, formed.²⁶ Since the molar volumes were in the order of Cu < Cu₂O < CuO, stresses were generated in the samples. The Cu₂O layer suffered compression from Cu on its bottom surface and tension from CuO on its top surface, while the CuO layer suffered compression from Cu₂O on its bottom surface and had a stress-free top surface. Thus, the stress gradient was in the direction from the Cu/Cu₂O interface to the CuO surface (outward of the sample surface). The atomic flux that is caused by stress-induced migration can be described as²⁵

$$J = \frac{C\Omega D}{k_B T} \nabla \sigma, \quad (1)$$

where C is the atomic concentration, Ω is the atomic volume, k_B is Boltzmann's constant, T is the absolute temperature, D is the local diffusion coefficient, and σ is the hydrostatic stress (average normal stress). It can be seen from Eq. (1) that the gradient of hydrostatic stress can serve as the driving force for atomic diffusion and the atomic flux is in the direction from more compressive/less tensile area to less compressive/more tensile area. Therefore, with the formation of Cu₂O and CuO layers, Cu ions migrated from the Cu/Cu₂O interface to the sample surface due to the stress-induced grain boundary diffusion, as shown in Fig. 7(e). These migrating ions served as the continuous source for the formation of CuO nanowires.

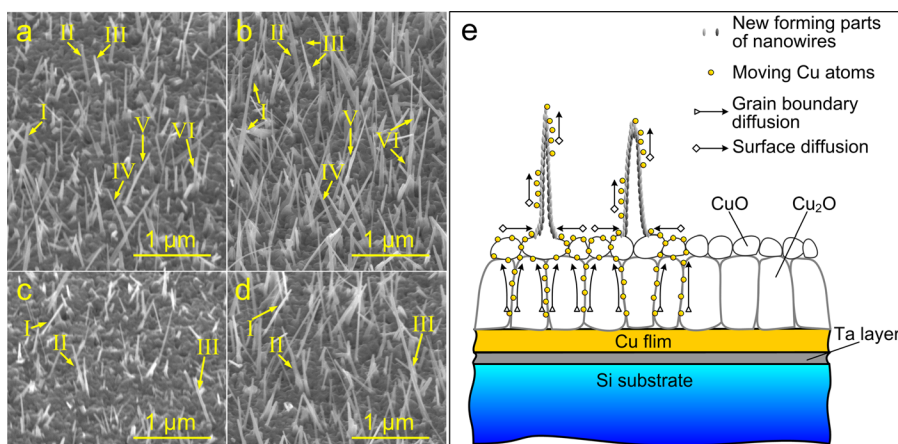


FIG. 7. Growth process of CuO nanowires. (a) and (c) SEM images of nanowires taken after heating the sample for 10 min. (b) and (d) SEM images taken from the same places as (a) and (c), respectively, after heating the sample for 30 min. The Cu film sample was heated at 350 °C. (e) Illustration of the FOOS mechanism for CuO nanowire growth.

When the Cu ions arrived at the sample surface, they continued to migrate to some specific sites through surface diffusion and initiated the growth of CuO nanowires. It was noted from Figs. 7(a) and 7(c) that most CuO nanowires initiated on the surfaces of CuO grains rather than out of the grain boundaries, which were in consistent with the statement made in Ref. 26. The driving forces for the surface diffusion were assumed to be the concentration gradient of the Cu ions and the local stress gradient on a microscopic level due to the material singularities.²⁵ After the initiation of nanowires, the subsequently arriving Cu ions climbed along the sidewalls of the nanowires, as illustrated in Fig. 7(e). The uneven nanowire surface (V in Fig. 7(b)) was an evidence of this climbing process. During the climbing process, the Cu ions might be incorporated into the CuO nanowires by reacting with the oxygen. This is the reason why the nanowires grew not only longer but also thicker with the increase of the heating time. It should be mentioned that, heating Cu foil at 400 °C for more than 2 h generated much longer nanowires than heating Cu thin film under the same condition (comparison between Figs. 3(c) and 4(c)). The reason is that the 400 nm thick Cu film was totally oxidized after being heated for a long time, and thereby the stress gradient which was the driving force for Cu ion migration tended to disappear. Another reason is the lack of Cu ion source in the Cu thin film.

C. Examination on components of the nanowires

To examine the components of the nanowires, individual nanowires were separated from the substrates and collected on the TEM observation grid. The TEM images and EELS spectra were obtained from the individual nanowires and shown in Fig. 8.

As shown in Fig. 8(a), the surface of the nanowire collected from the Al film sample was straight and smooth. The lattice fringe spacing shown in Fig. 8(b) was measured to be approximately 0.230 nm, which corresponded to the {111} plane of the Al crystal. It was also noticed from Fig. 8(b) that there was a 2 nm thick layer (without clear fringe) surrounding the Al nanowire. This thin layer was deduced to be

Al₂O₃ since pure Al is easy to be oxidized in air and forms a thin but dense surface layer to prevent further oxidation. The EELS spectrum shown in Fig. 8(c) confirmed that the main component of this nanowire was the Al metal. A CuO nanowire with diameter of 50 nm was shown in Fig. 8(d). The lattice fringe spacing shown in Fig. 8(e) was measured to be approximately 0.253 nm, which corresponded to the {002} plane of the CuO crystal. The EELS spectrum shown in Fig. 8(f) corresponded well with the typical CuO spectrum, which further confirmed that the main component of this nanowire was CuO.

The component examination supported that the nanowires growing from the Al film were Al nanowires, while those growing from the Cu film and Cu foil were CuO nanowires. This conclusion was consistent with our interpretations on the EAFB and FOOS growth mechanism.

D. Nanowires growing on patterned Cu film

As mentioned in Sec. III B, it was the stresses generated by the formation of Cu₂O and CuO that dominated the growth of CuO nanowires. However, in the case of Cu film sample, compressive stresses were also induced in the Cu film due to the thermal expansion mismatch between Cu film and Si substrate. In this section, the influence of such stresses on the growth of CuO nanowires was investigated.

In our experiment, it was observed that CuO nanowires preferred to grow on the edge of the patterned Cu film, as shown in Fig. 9(a). To interpret this phenomenon, finite element (FE) simulation was carried out to obtain the distribution of compressive stresses in Cu film, which were induced by the thermal expansion mismatch between Cu film and Si substrate.

To simplify the calculation without loss of correctness, the patterned Cu film-substrate system was modeled as follows. A Ta disc of 10 μm in diameter and 60 nm in height was placed on a Si substrate. Then a Cu column (patterned Cu film) of 10 μm in diameter and 400 nm in height was placed on the Ta disc. Young's moduli of 110, 185, and 150 GPa, Poisson's ratios of 0.34, 0.34, and 0.28, and

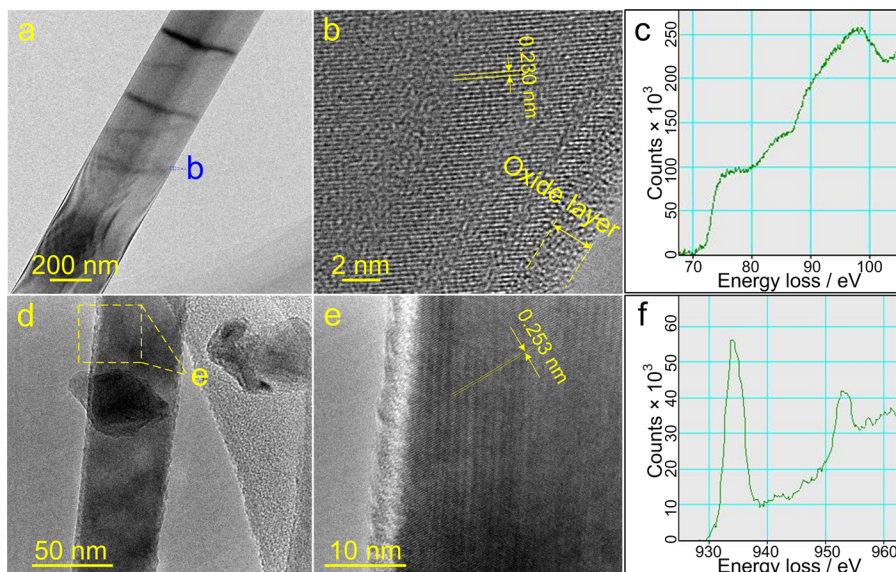


FIG. 8. TEM and EELS results of the individual nanowires. (a) TEM image of an Al nanowire. (b) High resolution TEM image from a part of the nanowire shown in (a). (c) EELS spectrum of the Al nanowire. (d) TEM image of a CuO nanowire. (e) High resolution TEM image from a part of the nanowire shown in (d). (f) EELS spectrum of the CuO nanowire.

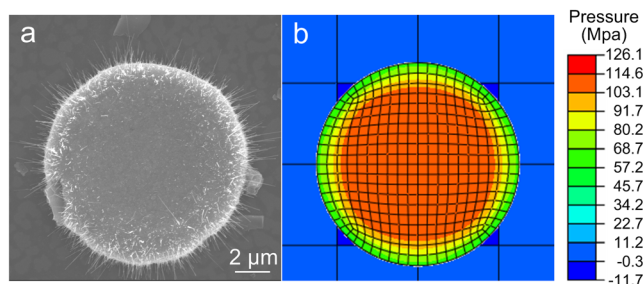


FIG. 9. The relationship between growth of CuO nanowires and the stresses induced by thermal expansion mismatch. (a) Nanowires growing on patterned Cu film. (b) Distribution of the compressive stresses obtained by the FE simulation.

thermal expansion coefficients of $16.5 \times 10^{-6} \text{ K}^{-1}$, $6.3 \times 10^{-6} \text{ K}^{-1}$ and $2.6 \times 10^{-6} \text{ K}^{-1}$ were adopted for Cu, Ta, and Si, respectively. Tie constraint was adopted as the boundary condition between every two adjacent layers. It can be estimated that Cu and Ta may experience the plastic deformation due to the great difference between the thermal expansion coefficients of metal and the Si substrate. Therefore, the ideal elastic-plastic constitutive relation was adopted for Cu and Ta in this study, and the yield stress was set to be 170 MPa. The initial temperature of the model was set to be 298 K. Then, the temperature was elevated to 623 K. The temperature was assumed to be uniformly applied to the model according to the experimental condition. In fact, only the stress status at the elevated temperature of 623 K was calculated.

As can be seen from Fig. 9(b), the radial distribution of hydrostatic stress on the top surface of the Cu column is in such a way that it is less pressed on the edge than in the center. The stress gradient is in the direction from the center of the Cu column to its edge. Thus, according to Eq. (1), Cu ions tend to migrate along the stress gradient to the less pressed edge of the patterned Cu film. This is the reason why CuO nanowires preferred to grow on the edge of the patterned Cu film. In a very recent paper, it was also reported that CuO nanowires preferred to grow on the tensile surface of a bended Cu foil.²⁷ Thus, it can be further deduced that although the growth of metal oxide nanowires is dominated by stresses that arise due to the formation of metal oxide layers, stress distribution on the macroscopic level, which is caused by thermal or mechanical manipulation also influences the growth situation. It is prospective to control the growth of metal oxide nanowires by designing the stress distribution within the sample from which the nanowires are generated.

IV. CONCLUSION

In conclusion, we studied the growth mechanism of metal and metal oxide nanowires through implementing the growth of Al and CuO nanowires by simply heating the Al and Cu samples in air. Although the experimental operations and the stress-induced migration processes were quite similar, the causes of the driving forces and the growth mechanism

were completely different. For the growth of metal (Al) nanowires, the driving force was determined to be the compressive stresses caused by the thermal expansion mismatch between metal film and Si substrate, and the growth mechanism was proposed to be the extrusion of atoms from the bases of nanowires (EAFB). For the growth of metal oxide (CuO) nanowires, the driving force was determined to be the compressive stresses caused by the formation of metal oxide layers, and the growth mechanism was proposed to be the formation of oxide molecules on surfaces of the nanowires (FOOS). The direct experimental observations of both EAFB and FOOS were presented. It was also demonstrated that although the growth of metal oxide nanowires was dominated by stresses that arose due to the formation of metal oxide layers, stress distribution on the macroscopic level, which was caused by thermal or mechanical manipulation also influenced the growth situation. It is prospective to control the growth of metal oxide nanowires by designing the stress distribution within the sample from which the nanowires are generated.

¹M. Law, L. E. Greene, J. C. Johnson, R. Saykally, and P. Yang, *Nature Mater.* **4**, 455 (2005).

²Y. W. Zhu, C. H. Sow, and J. T. L. Thong, *J. Appl. Phys.* **102**, 114302 (2007).

³J. Chen, K. Wang, L. Hartman, and W. Zhou, *J. Phys. Chem. C* **112**, 16017 (2008).

⁴X. C. Jiang, T. Herricks, and Y. N. Xia, *Nano Lett.* **2**, 1333 (2002).

⁵A. Kumar, A. K. Srivastava, P. Tiwari, and R. V. Nandedkar, *J. Phys. Condens. Matter* **16**, 8531 (2004).

⁶M. Kaur, K. P. Muthe, S. K. Deshpande, S. Choudhury, J. B. Singh, N. Verma, S. K. Gupta, and J. V. Yakhmi, *J. Cryst. Growth* **289**, 670 (2006).

⁷N. Chopra, B. Hu, and B. J. Hinds, *J. Mater. Res.* **22**, 2691 (2007).

⁸A. M. B. Goncalves, L. C. Campos, A. S. Ferlauto, and R. G. Lacerda, *J. Appl. Phys.* **106**, 034303 (2009).

⁹M. L. Zhong, D. C. Zeng, Z. W. Liu, H. Y. Yu, X. C. Zhong, and W. Q. Qiu, *Acta Mater.* **58**, 5926 (2010).

¹⁰Y. Wang, R. Shen, X. Jin, P. Zhu, Y. Ye, and Y. Hu, *Appl. Surf. Sci.* **258**, 201 (2011).

¹¹F. Mumm and P. Sikorski, *Nanotechnology* **22**, 105605 (2011).

¹²Y. Yue, M. Chen, Y. Ju, and L. Zhang, *Scripta Mater.* **66**, 81 (2012).

¹³J. M. Cowley, *J. Electrochem. Soc.* **101**, 277 (1954).

¹⁴R. Takagi, *J. Phys. Soc. Jpn.* **12**, 1212 (1957).

¹⁵E. A. Gulbransen, T. P. Copan, and K. F. Andrew, *J. Electrochem. Soc.* **108**, 119 (1961).

¹⁶S. Ren, Y. F. Bai, J. Chen, S. Z. Deng, N. S. Xu, Q. B. Wu, and S. H. Yang, *Mater. Lett.* **61**, 666 (2007).

¹⁷A. G. Nasibulin, S. Rackauskas, H. Jiang, Y. Tian, P. R. Mudimela, S. D. Shandakov, L. I. Nasibulina, J. Sainio, and E. I. Kauppinen, *Nano Res.* **2**, 373 (2009).

¹⁸I. A. Blech, P. M. Petroff, K. L. Tai, and V. Kumar, *J. Cryst. Growth* **32**, 161 (1975).

¹⁹K. Hinode and Y. Homma, *J. Vac. Sci. Technol. A* **14**, 2570 (1996).

²⁰J. W. Lee, M. G. Kang, B. S. Kim, B. H. Hong, D. Whang, and S. W. Hwang, *Scripta Mater.* **63**, 1009 (2010).

²¹H. Tohmyoh, M. Yasuda, and M. Saka, *Scripta Mater.* **63**, 289 (2010).

²²W. Lee, W. Shim, J. Ham, K. I. Lee, W. Y. Jeung, and M. Johnson, *Nano Lett.* **9**, 18 (2009).

²³J. Ham, W. Shim, D. H. Kim, K. H. Oh, P. W. Voorhees, and W. Lee, *Appl. Phys. Lett.* **98**, 043102 (2011).

²⁴W. Shim, J. Ham, J. S. Noh, and W. Lee, *Nanoscale Res. Lett.* **6**, 196 (2011).

²⁵M. Saka, F. Yamaya, and H. Tohmyoh, *Scripta Mater.* **56**, 1031 (2007).

²⁶L. Yuan, Y. Wang, R. Mema, and G. Zhou, *Acta Mater.* **59**, 2491 (2011).

²⁷R. Mema, L. Yuan, Q. Du, Y. Wang, and G. Zhou, *Chem. Phys. Lett.* **512**, 87 (2011).